The Optical Soliton Transmission Amplified by Bidirectional Raman Pumps with Nonconstant Depletion

Senfar Wen, Tsun-Yee Wang, and Sien Chi

Abstract—**A numerical method is proposed to solve the coupled equations between the soliton and bidirectional Raman pump waves. The pump depletion due to the soliton is obtained without using the constant depletion approximation. With this method, the soliton propagation in a Raman-pumped fiber can be solved accurately. It is found that the constant depletion approximation is valid at a small depletion rate, which requires low soliton power (or long pulsewidth), small material loss, and a short-pump period. In a periodically Raman-pumped fiber, there exists a stable signal energy, which is very sensitive to the pump intensity. We have also studied the stability of the soliton propagation with nonconstant pump depletion. It is found that the stability predicted by nonconstant depletion (NCD) and constant depletion assumption (CDA) are generally different.**

I. Introduction

THE OPTICAL soliton has been proposed as a dispersionless carrier for high-bit-rate fiber communication systems [1]. In a lossy fiber, the soliton disperses. To compensate the fiber loss in long distance transmission, periodically bidirectional Raman pumps were proposed and proved to be an effective method to compensate the loss and maintain the pulse shape of the soliton [2], [3].

The theoretical study of the system amounts to solve the coupled equations between the soliton and Raman pump waves. In the literature, the depletion of the pump wave by the soliton is often assumed to be a constant or to be ignored [2], [3]. The constant depletion approximation (CDA) is valid when the depletion and the variation of the soliton energy are small and the relative velocity between the soliton and the pump wave is large. For the small relative velocity, the local interaction between the soliton and the pump wave can not be ignored and changes the pulse shape of the soliton [4]. In this paper, we propose a new numerical method to solve the coupled equations when large relative velocities are involved. With this method, the pump depletion is accurately predicted and the soliton transmission in the Raman pumped fiber can be studied in a wide range.

Manuscript received December 4, 1990; revised April 4, 1991. This work was supported by National Science Council, Republic of China, under Contract NSC 80-0417-E-009-13.

The authors are with the Institute of Electro-Optical Engineering and Center for Telecommunications Research, National Chiao Tung University, Taiwan 30050, R.O.C.

IEEE Log Number 9101360.

II. Coupled Wave Equations and the Numerical Method

The soliton and the forward Raman pump wave in a fiber satisfy the following coupled dimensionless wave equations [2], [4]:

$$i\frac{\partial q_s}{\partial \xi} + \frac{1}{2}\alpha_s\frac{\partial^2 q_s}{\partial \tau^2} + \eta_s(|q_s|^2 + 2|q_p|^2)q_s = -i\Gamma_s q_s + iG|q_p|^2 q_s \tag{1}$$

$$i\left(\frac{\partial q_p}{\partial \xi} - V\frac{\partial q_p}{\partial \tau}\right) - \frac{1}{2}\alpha_p\frac{\partial^2 q_p}{\partial \tau^2} + \eta_p(|q_p|^2 + 2|q_s|^2)q_p = -i\Gamma_p q_p - i\kappa G|q_s|^2 q_s \tag{2}$$

where the variables and the coefficients are normalized in the following way:

$$\xi = X^{-1}z, \qquad \tau = T^{-1}(t - k_s' z),$$
$$q_s = Q^{-1}\phi_s, \qquad q_p = Q^{-1}\phi_p \tag{3}$$

and

$$\alpha_s = -k_s'' XT^{-2}, \qquad \alpha_p = k_p'' XT^{-2}$$
$$\eta_s = \frac{\pi n_2}{\lambda_s}Q^2 X, \qquad \eta_p = \frac{\pi n_2}{\lambda_f}Q^2 X$$
$$\Gamma_s = \gamma_s X, \qquad \Gamma_p = \gamma_p X, \qquad G = \frac{n_0}{4}\sqrt{\epsilon_0/\mu_0}\, gXQ^2$$
$$V = (k_p' - k_s')XT^{-1}, \qquad \kappa = \frac{\lambda_s}{\lambda_p}. \tag{4}$$

In (1)–(4), ϕ_s and ϕ_p are the electric field envelopes of the soliton and the forward pump wave; λ_s and λ_p are the wavelengths of the soliton and the pump wave; t and z are the time and propagation distance along the fiber; T, X, and Q are the time, distance, and electric field scale factors; k_s', k_s'' and k_p', k_p'' are the derivatives of the propagation constant k with respect to the angular frequencies evaluated at ω_s and ω_p, respectively, ω_s and ω_p are the angular frequencies of the soliton and the pump wave, the first derivative is reciprocal group velocity, the second derivative is proportional to the group dispersion; γ_s and γ_p are the loss coefficients of the fiber at λ_s and λ_p; n_2 is the Kerr coefficient and equals to 1.22×10^{-22} $(V/m)^{-2}$

for fused silica; g is the Raman gain coefficient which is maximum when the frequency difference between pump wave and the carrier wave of soliton is 440 cm^{-1} [5]. The maximum gain $g = 9.75 \times 10^{-14}/\lambda_p$ (m/W) where λ_p is in the unit of microns.

We define the soliton energy as

$$E = \int_{-(\Delta\tau/2)}^{\Delta\tau/2} |q_s|^2 \, d\tau \tag{5}$$

where $\Delta\tau$ is the period of q_s, and forward pump intensity $I_f = |q_p|^2$. By assuming the periodical boundary condition and large relative velocity between the soliton and the pump wave, (1) and (2) can be reduced to

$$\frac{\partial E}{\partial \xi} + 2(\Gamma_s - GI_f)E = 0 \tag{6}$$

$$\frac{\partial I_f}{\partial \xi} + 2\left(\Gamma_p + \frac{\kappa G}{\Delta\tau} E\right) I_f = 0. \tag{7}$$

Note that $E/\Delta\tau$ is the soliton's average intensity. The coupled equations, (6) and (7), can be analytically solved for $\Gamma_s = \Gamma_p$ [6]. In the following, we consider a numerical method to solve the coupled equations without assuming $\Gamma_p = \Gamma_p$. Furthermore, both forward and backward pump waves can be solved simultaneously by this method.

From (7), we have the forward pump intensity

$$I_f(\xi) = I_{fo} \exp[-\rho_f \xi] \tag{8}$$

where $I_{fo} = I_f(\xi = 0)$ is the initial forward pump intensity and

$$\rho_f = 2\Gamma_p + \frac{2\kappa G}{\Delta\tau} \bar{E}_f \tag{9}$$

is the forward pump loss rate where

$$\bar{E}_f = \frac{1}{\xi} \int_0^{\xi} E \, d\xi \tag{10}$$

is the forward mean soliton energy from the initial to the present position. On the right-hand side of the equal sign in (9), the first term is the material loss rate at the pump wavelength and the second term is the pump depletion loss rate. The pump depletion loss rate depends not only on the present soliton energy but also on the history of the soliton as the definition of $\bar{E}_f$ in (10) shows. This indicates that the pump intensity at ξ depends on how the pump wave is depleted from $\xi = 0$. To consider bidirectional pumps, we assume the fiber length to be ξ_o and the backward pump wave is injected into the fiber from ξ_o.

Similarly, we have the backward pump intensity

$$I_b(\xi) = I_{bo} \exp[\rho_b(\xi - \xi_o)] \tag{11}$$

where $I_{bo} = I_b(\xi = \xi_o)$ is the initial backward pump intensity and

$$\rho_b = 2\Gamma_p + \frac{2\kappa G}{\Delta\tau} \bar{E}_b \tag{12}$$

is the backward pump loss rate where

$$\bar{E}_b = \frac{1}{(\xi_o - \xi)} \int_{\xi}^{\xi_o} E \, d\xi \tag{13}$$

is the backward mean soliton energy.

Therefore, the coupled equation for the soliton energy and total pump intensity become

$$\frac{\partial E}{\partial \xi} + 2(\Gamma_s - GI)E = 0 \tag{14}$$

$$I = I_{fo} \exp[-\rho_f \xi] + I_{bo} \exp[\rho_b(\xi - \xi_o)] \tag{15}$$

where the coupling is through E contained in ρ_f and ρ_b. Because only the energy relation is considered in (14) and (15), the coupled equations can be applied to the Raman amplification problem discussed in [6].

We solve (14) and (15) by the iterative method. From (14), we have the iteration formula

$$E(\xi + \Delta\xi) = E(\xi) \exp[2(-\Gamma_s + GI(\xi))\,\Delta\xi]. \tag{16}$$

From (9), (12), (15), and (16), with the initial soliton energy $E_o = E(\xi = 0)$ we obtain the first step soliton energy solution $E^{(1)}(\xi)$. In the first step, $\bar{E}_f$ and $\bar{E}_b$ are taken to be $\bar{E}_f(\xi) = E(\xi)$ and $\bar{E}_b(\xi) = E(\xi)$ rather than their original definitions in (10) and (13) because $\bar{E}_b(\xi)$ can not be calculated unless E along ξ is previously known. $\bar{E}_f(\xi)$ and $\bar{E}_b(\xi)$ are taken to be their original definitions in the following iterative steps because the approximate soliton energy along the fiber is obtained. Substituting $E^{(1)}(\xi)$ into the iterative equations, we have the second step soliton energy soliton $E^{(2)}(\xi)$. The iterative process repeats until the mean error

$$\epsilon = \left\{ \frac{1}{\xi_o} \int_0^{\xi_o} [E^{(m)} - E^{(m-1)}]^2 \, d\xi \right\}^{1/2}$$

of the mth step is below a tolerable value. From the final step solution $E^{(m)}$, both the forward and backward pump depletion loss rates can be obtained. Therefore the coupled equations for the soliton and the pump waves are reduced to (15) and

$$i\frac{\partial q}{\partial \xi} + \frac{1}{2}\alpha \frac{\partial^2 q}{\partial \tau^2} + \eta |q|^2 q = -i\Gamma q + iGIq \tag{17}$$

where the subscript s for the soliton is dropped.

Equation (17) can be numerically solved by the beam-propagating method [7]. The method assumes the periodic boundary condition, and $\Delta\tau$ in (5) is the period. The initial condition to solve (17) is taken to be

$$q(\tau, \xi = 0) = \mu\sqrt{\alpha/\eta}\ \mathrm{sech}\,(\mu\tau), \quad -\frac{\Delta\tau}{2} \le \tau < \frac{\Delta\tau}{2} \tag{18}$$

where μ is an arbitrary constant, q is the fundamental soliton with amplitude $\mu\sqrt{\alpha/\eta}$ and pulsewidth (FWHM) $T_w = 1.76T/\mu$(ps). Note that, from (4) and (18), the pulse amplitude is inversely proportional to the time scale T. In this paper, the period $\Delta\tau$ is taken to be $35.2/\mu$(20 pulse-

widths separation). The initial soliton energy $E_o = 2\pi\alpha/\eta$.

For periodically bidirectional pumps, it is generally assumed that the pump waves of equal intensity are injected at each distance of ξ_p into the fiber in both directions that along and against the direction of the soliton propagation. Then the pump intensity at the nth pump period is

$$I = I_o(\exp\{-\rho_f[\xi - (n-1)\xi_p]\} + \exp\{\rho_b[\xi - n\xi_p]\}), \quad n = 1, 2, 3 \cdots \quad (19)$$

where I_o is the injected pump intensity. The pump loss rates ρ_f and ρ_b are obtained by the iterative method with the initial soliton energy

$$E_{no} = \int_{-(\Delta\tau/2)}^{\Delta\tau/2} |q(\tau, \xi = (n-1)\xi_p)|^2 \, d\tau.$$

The coupling loss from a pump period to the next period is neglected for simplicity.

III. Comparison with the Case of Constant Depletion Assumption

In this section, we will work out some examples with the numerical method shown in last section and check the validity of the CDA. The CDA is valid when [2]

$$\Gamma\xi_p \ll 1 \quad (20)$$

then the pump loss rates in (19) can be taken as

$$\rho_f = \rho_b = \rho_c = 2\Gamma_p + \frac{2\kappa G}{\Delta\tau} E_{no} \quad (21)$$

where E_{no} is the initial soliton energy at the nth pump period and ρ_c is in fact the pump loss rate at $\xi = (n-1)\xi_p$. When the condition (20) is valid, the attenuation of the soliton is small. This leads to a small variation of the soliton energy when the fiber loss is compensated by the Raman pump. To compensate the fiber loss within a pump period, the integrated gain from the pump waves must be equal to the integrated fiber loss ($2\Gamma\xi_p$). The integrated gain for the nth pump period is $4I_oG/\rho_c\,[1 - \exp(-\rho_c\xi_p)]$. Therefore, the required initial pump intensity to compensate the fiber loss is [2]

$$I_o = \frac{\rho_c\Gamma\xi_p}{2G[1 - \exp(-\rho_c\xi_p)]}. \quad (22)$$

However, the condition (20) is not valid for the interested range of parameters. For the minimum fiber loss 0.2 dB/km and 40 km pump period, $\Gamma\xi_p = 0.92$ does not satisfy (20). By the following numerical examples, it is shown that CDA can be applied well even if (20) is not satisfied.

In the following, we take $\lambda_s = 1.55$ μm and $\lambda_p = 1.46$ μm. The fiber losses are taken to be $\gamma_s = 0.3$ dB/km and $\gamma_p = 0.5$ dB/km. The dispersion at the soliton wavelength is taken to be 2 ps/km/nm which corresponds to $k_s'' = -2.55$ ps^2/km. Taking $\alpha = 1$, $\eta = 1$, and $X = 10$ km in (4), we have the scale factors $T = 5.0$ ps and $Q = 6.36 \times 10^5$ V/m. For the 25 μm^2 effective cross section of fiber core, the given electric field scale factor Q corresponds to 20.0 mW power scale factor. The other coefficients in (15) and (19) are $\Gamma = 0.345$, $\Gamma_p = 0.576$, $= 0.26$, and $\kappa = 1.06$. The numerical values given here are used throughout this paper except specially specified.

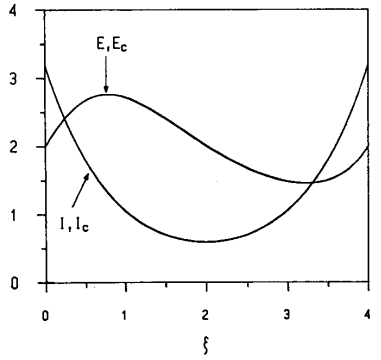

Fig. 1. Soliton energies E and E_c and pump intensities I and I_c versus distance ξ for $\mu = 1$, $\xi_p = 4$, and $I_o = 3.1682$. It is noticed that the curves for E and E_c are almost overlapped, so are the curves for I and I_c.

With the initial condition given by (18), I_o given by (22), and the coefficients given above, we solve (17), (14), and (19). Fig. 1 shows the soliton energy E and pump intensity I with respect to distance ξ for $\mu = 1$ and $\xi_p = 4$ (40 km). In Fig. 1, the soliton energy (E_c) and pump intensity (I_c) obtained by CDA are also plotted. Fig. 2 shows the depletion loss rates of the pump waves. We define the depletion loss rate $\sigma_j = 2\kappa G\bar{E}_j/\Delta\tau$, $j = f, b$. The depletion loss rate obtained by CDA, $\sigma_c = 2\kappa GE_o/\Delta\tau$, is also shown in Fig. 2 where σ_c is in fact the initial depletion loss rate. From Fig. 1, it is seen that the two sets of curves are almost overlapped. Because the evolution of E is almost the same as E_c, the evolution of q is also. This shows, in this case, that CDA is applied well although $\Gamma\xi_p = 1.38$ and (20) are not satisfied. With the initial pump intensity given by (22), the soliton energy calculated by CDA recovers to its initial energy at $\xi = \xi_p/2$ and ξ_p. In this numerical example, the soliton energy is very close to the initial energy as is expected by CDA; $E(\xi = 2) = 1.990$ and $E(\xi = 4) = 1.997$. In Fig. 2, $\sigma_c = 0.031$; σ_f is larger than σ_c because the soliton is amplified from the beginning and the forward pump wave is more seriously depleted than at the beginning. At the end of the pump period $\xi = \xi_p$, σ_f is still larger than σ_c; this indicates the mean soliton energy over the pump period is slightly larger than E_o. As to the backward pump wave, the soliton energy is less than E_o within the back half pump period so σ_b is less than σ_c · $\sigma_b(\xi = 0)$ is equal to $\sigma_f(\xi = \xi_p)$ since both $\bar{E}_b(\xi = 0)$ and $\bar{E}_f(\xi = \xi_p)$ are the mean soliton energy over the pump period. We define $\sigma_o = \sigma_f(\xi = \xi_p) = \sigma_b(\xi = 0)$. It is found that, if $\sigma_o > \sigma_c$, $E(\xi = \xi_p) < E_c(\xi = \xi_p)$, and vice versa. In Fig. 2, $\sigma_o = 0.032$ is larger than σ_c and, in Fig. 1, $E(\xi = 4) < E_c(\xi = 4)$. This is because larger σ_o means larger mean soliton energy over the period and leads to higher depletion. In next numerical example, we will show that $E(\xi = \xi_p) >$

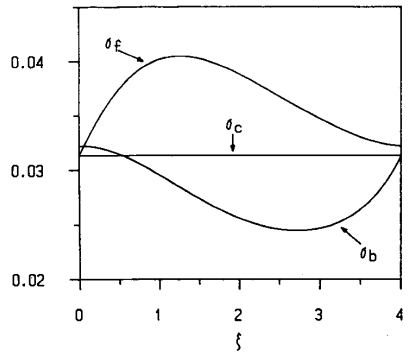

Fig. 2. Forward and backward depletion loss rates (σ_f and σ_b) in Fig. 1.

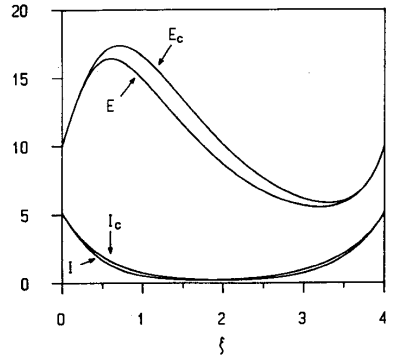

Fig. 3. Soliton energies E and E_c and pump intensities I and I_c versus distance ξ for $\mu = 5$, $\xi_p = 4$ and $I_o = 5.1373$.

$E_c(\xi = \xi_p)$ when $\sigma_o < \sigma_c$. In Fig. 2, maximum $\sigma_f = 0.0405$ and minimum $\sigma_b = 0.0245$. It is noticed that the material loss rate $2\Gamma_p$ is 1.152 which is much larger than σ_f and σ_s. This is the reason why CDA is applied well in this case. For

$$2\Gamma_p \gg \sigma_f, \sigma_b \tag{23}$$

the contribution of the pump loss rates from the pump depletion can be neglected.

Fig. 3 shows an example with the same parameters as Fig. 1 except $\mu = 5$. For $\mu = 5$, $\sigma_c = 0.783$ which is close to $2\Gamma_p$. Equation (23) is not satisfied in this case and it is expected that CDA is invalid. The invalidity can be clearly observed in Fig. 3. Fig. 4 shows the pump depletion loss rates in Fig. 3 where maximum $\sigma_f = 1.168$, minimum $\sigma_b = 0.497$, and $\sigma_o = 0.7815$ which is less than σ_c. For $\sigma_o < \sigma_c$, it is expected that $E(\xi = \xi_p) > E_c(\xi = \xi_p)$ as discussed above. In Fig. 3, along the fiber E is almost less than E_c every where except at the last section where E is pumped to catch up with E_c and is larger than E_c finally. At the end of the pump period, $E(\xi = 4) = 10.10$ which is slightly larger than $E_c(\xi = \xi_p) = E_o = 10$. The soliton energy recovers to its initial energy at $\xi = 1.737$ and 3.995. Fig. 5 shows the envelope of $|q|$ at $\xi = \xi_p$ where the envelope obtained by CDA is also plotted. It is seen that the peak amplitude of the envelope at $\xi = \xi_p$ is slightly larger than the result obtained by CDA. The different evolutions lead to different envelopes at the end of the pump period after propagating several pump periods. We will consider the envelope evolutions in Section V.

The soliton considered in Fig. 1 ($\mu = 1$) is initially with 8.8 ps pulsewidth and 20 mW peak power. The soliton considered in Fig. 3 ($\mu = 5$) is initially with 1.76 ps pulsewidth and 500 mW peak power. The more soliton power, the more pump wave is depleted. High depletion loss rate leads to the invalidity of CDA. For CDA to be valid, the soliton power along the fiber must all be small enough. For large Γ and/or Γ_p, the soliton needs to be greatly amplified from the beginning to endure high loss in the middle of the pump period where the pump intensity is small. The same is true in the case of a very long pump period. These conditions may cause high soliton power and high depletion loss rate some where in the fiber and make CDA invalid. Fig. 6 shows the case with the same parameters as in Fig. 3 except Γ_p is increased up to 4.032 (3.5 dB/km). In Fig. 6, $2\Gamma_p$ is about ten times greater than σ_c, but the deviation of the solution from that obtained by CDA is more serious than the deviation in Fig. 3. The soliton energy at the end of the pump period is 9.62.

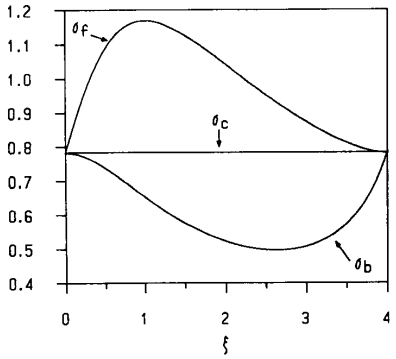

Fig. 4. Forward and backward depletion loss rates (σ_f and σ_b) in Fig. 3.

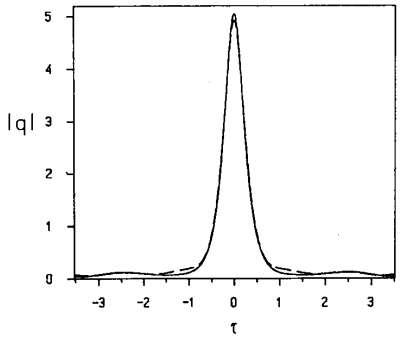

Fig. 5. Envelopes of the soliton ($|q|$) for $\mu = 1$, $\xi_p = 4$, and $I_o = 3.1682$ at $\xi = \xi_p$. The envelope of the soliton obtained by CDA is also shown by dashed line for comparison.

In this section, only one pump period is considered. After propagating several pump periods, the error resulted

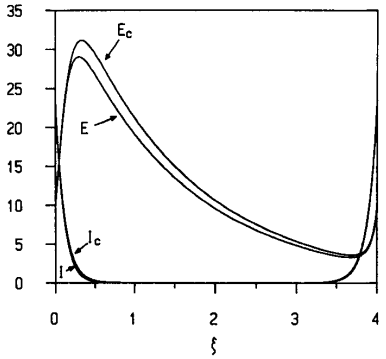

Fig. 6. Soliton energies E and E_c and pump intensities I and I_c versus distance ξ for $\mu = 5$, $\xi_p = 4$, $\Gamma_p = 4.032$, and $I_o = 23.4785$.

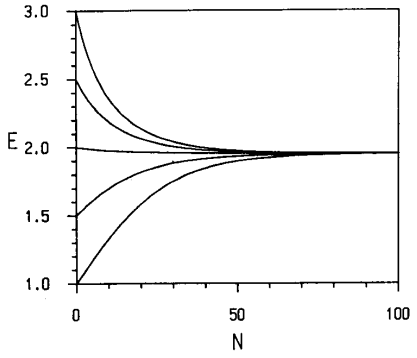

Fig. 7. Signal energies (E) at the end of the Nth pump period for various initial signal energies with $\mu = 1$, $\xi_p = 4$, and $I_o = 3.1682$. The initial signal energies are shown at $N = 0$. The signal energies all approach to $E = 1.951$.

from assuming CDA should accumulate. In the next section, it is shown that the error of the soliton energy at the end of a pump period reaches a stable value. For the practical soliton-based communication system [3], the material loss at soliton wavelength and pump wavelength is about 0.2 dB/km, and the solition pulsewidth is larger than 10 ps, and the pump period is less than 50 km. It is found that, for these data, CDA is valid for the communication system.

IV. Stable Signal Energy in the Periodically Raman-Pumped Fiber

In Section III, the initial soliton is exactly the fundamental soliton; the pump power is given by (22) which is designed to compensate the fiber loss exactly under CDA; only the propagation in the first pump period is considered. In the followings, we will study more general cases. The initial soliton is not necessary the fundamental soliton or the initial pump intensity is not necessarily given by (22). In this section, we will study the evolution of the soliton energy for several pump periods.

In this section, we solve the coupled equations of the soliton energy and pump intensity, (14) and (19). It is noticed that the energy increment is in fact not necessarily equal to the increment of the soliton energy. The energy increment may be radiated away from the soliton due to the combined effect of the dispersion and the Kerr effect. Furthermore, the radiated wave is amplified by the Raman pumps and shares the energy increment.

In the following, the coefficients are the same as in Fig. 1. Fig. 7 shows the signal energies at the end of every pump period for various initial signal energies. For different initial signal energies E_i, the corresponding initial pump intensities are set to be the same and given by (22) with $E_o = 2$ in $\rho_c \cdot I_o = 3.1682$. In Fig. 1 ($E_i = 2$), at the end of the first pump period, the energy is 1.997. From Fig. 7, it is seen that, after propagating several tens of pump periods, the energy at the end of a pump period reaches the stable value 1.951. For different initial signal energies, the energies all reach the same value. This can be easily realized that the initial pump intensity $I_o = 3.1682$ completely compensates the fiber loss of the signal with $E_i = 1.951$. The stable energy with loss completely compensated is designed by E_{ss}. Both the signal with higher energy decays and the signal with lower energy grows to the same stable energy level.

Fig. 8 shows the signal energies at the end of every pump period for $E_i = 2$ and various I_o. For $I_o = 3.5$, the signal energy is pumped up to $E_{ss} = 9.985$. For $I_o = 3.1$, the signal energy decays to $E_{ss} = 0.292$. For $I_o = 3.0$, the signal energy decays to zero, i.e., the pump intensity can not compensate the fiber loss of the signal.

If CDA is valid, the relation of E_{ss} and I_o can be obtained by solving (22) where ρ_c is given by (21) and E_o is replaced by E_{ss}^c, where E_{ss}^c is the E_{ss} obtained from (22). In (22), the fiber loss of the soliton is completely compensated by Raman pumps. For $\rho_c \xi_p >> 1$, from (21) and (22) we have

$$\frac{E_{ss}^l}{\Delta\tau} = -\frac{\Gamma_p}{\kappa G} + \frac{1}{\kappa\Gamma\xi_p} I_o \tag{24}$$

where E_{ss}^l is the E_{ss} obtained under this approximation. Because there is no negative light power, E_{ss}^l becomes zero if it is negative by (24). Equation (24) shows the linear relation of E_{ss}^l and I_o. From (24), we see there is a threshold I_o to maintain the signal energy. This threshold I_o designated by I_{th}^l is $\Gamma\Gamma_p \xi_p / G$. The threshold value obtained by solving (14) and (19) is designated by I_{th} and by solving (22) is designated by I_{th}^c.

Figs. 9 and 10 show E_{ss} versus I_o. The range of I_o in Fig. 9 is from three to ten, while the range of I_o in Fig. 10 is from 3 to 3.5 to show the range that can not be clearly observed in Fig. 9. Near threshold pump intensity, E_{ss}^l is very different from E_{ss}^c. E_{ss}^l coincide with E_{ss}^c for $I_o > 5$. From the figures, we see $I_{\text{th}} = I_{\text{th}}^c = 3.08$ while $I_{\text{th}}^l = 3.06$. For $I_o < 4.66$, $E_{ss} < E_{ss}^c$, and, for $I_o > 4.66$, $E_{ss} > E_{ss}^c$. We let the pump intensity as I_{oe}, when $E_{ss} = E_{ss}^c$. As discussed in last section, the result shows $\sigma_o < \sigma_c$ for $I_o > 4.66$.

From Fig. 9, it is seen that a slight change of the pump intensity may cause a large change of the signal energy.

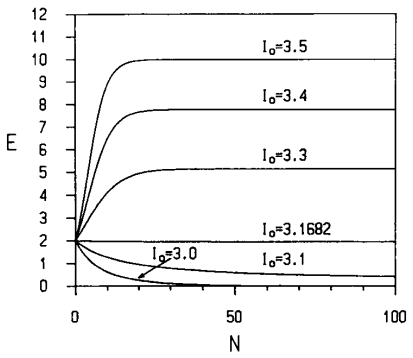

Fig. 8. Signal energies (E) at the end of the Nth pump period for the initial soliton energy $E_i = 2$ and various initial pump intensities I_o with $\mu = 1$ and $\xi_p = 4$.

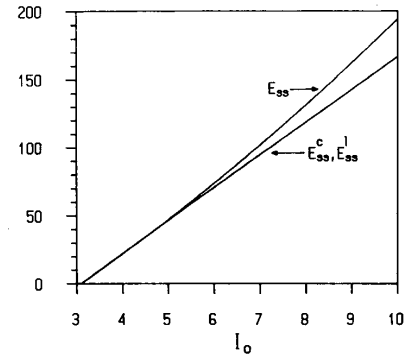

Fig. 9. Stable signal energy E_{ss} versus initial pump intensity for $I_o = 3$ to 10.

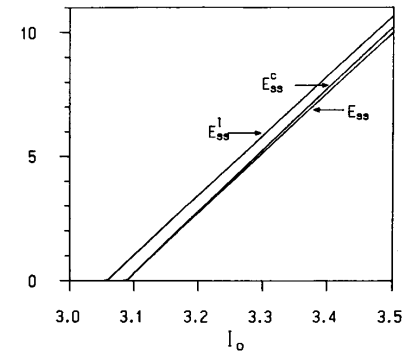

Fig. 10. Stable signal energy E_{ss} versus initial pump intensity for $I_o = 3$ to 3.5.

For example, $I_o = 3.1$ corresponds to $E_{ss} = 0.292$. If I_o is increased from 3.1 to 3.5, the signal energy is pumped up to 9.985. It is amplified about 34 times, while the pump intensity only change 1.13 times. Therefore, careful control of the pump power is necessary for the soliton-based communication systems. This effect can be observed by using the experimental apparatus set up in [8]. In the apparatus, a fiber is closed on itself with an all-fiber version of a Mach–Zehnder interferometer. The signal wave recirculates around the loop and the pump waves are injected into the loop bidirectionally.

V. Stability of the Soliton Propagation in the Periodically Raman-Pumped Fiber

In this section, we study the stability of the soliton propagation in periodically Raman pumped fiber with nonconstant depletion (NCD) and compare the results with the case of CDA. With CDA, the stability properties have been studied in [3]. It is found that the stability depends on the ratio of the perturbation period (the pump period $L = \xi_p X$) and the soliton period z_o. The soliton period is defined by

$$z_o = (\pi/2)\mu^{-2}X \tag{25}$$

where $X = (T^2/-k_s'')$. It is known that the fundamental soliton solution of (17) with $\alpha = \eta = 1$ and $\Gamma = G = 0$ is

$$q(\tau, \xi) = \mu \operatorname{sech}(\mu\tau) \exp[i(\mu^2/2)\xi]. \tag{26}$$

From (26), the soliton experiences a phase change of $\pi/4$ when it propagates z_o distance. It is found that the soliton is unstable for $L/z_o \cong 8$ because it corresponds to 2π phase change of the soliton when it propagates L distance and leads to a resonance between the perturbation period (L) and the soliton phase. The soliton is stable for $L/z_o << 1$ where the perturbation period is small compared with the soliton period.

The stability property can be represented by the relation of δS and L/z_o where δS is the ratio of the area change of the soliton at the end of the first pump period and is defined by

$$\delta S = [S(\xi_p) - S(0)]/S(0) \tag{27}$$

where the area of a soliton is defined by $S(\xi) = \int |q(\tau, \xi)| d\tau$.

Fig. 11 shows δS versus L/z_o for $L = 40$ km. The numerical values of the parameters are the same with those in Fig. 1 except μ is varied and initial pump intensity I_o is chosen to make the soliton energy recover at the end of the pump period. In (27), $S(0) = \pi$ nevertheless μ is varied. In Fig. 11, the dashed curve represents the result obtained by CDA, where the initial pump intensity I_o is given by (22). It is noticed that $L/z_o = 8\mu^2/\pi$. In Fig. 11, the horizontal axis represented by μ is also shown. We have known that CDA is valid only when μ is small as is discussed in Section III. It is seen that the two curves overlapped for μ less than about 1.5. For larger μ, the two curves are different and there are resonant peaks. The peaks are nearly at the multiples of 7.5 in unit of L/z_o for the curve with NCD. It is noticed that the peaks obtained by CDA are advanced with respect to those obtained by NCD. The resonant peaks can be explained as follows.

In (25), the soliton period z_o is, in fact, only valid in lossless fibers. In a Raman-pumped fiber, the amplitude of the soliton varies along the fiber. If the pulse shape of the soliton is maintained well, from (26) we can define the effective soliton amplitude as $\mu_e = \bar{E}/2$ where $\bar{E}$ is

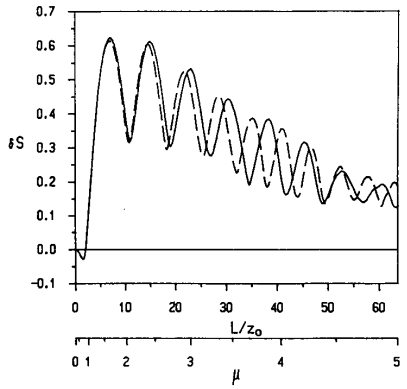

Fig. 11. Area change ratio of the soliton δS versus L/z_o and μ. δS obtained by CDA is shown by the dashed line.

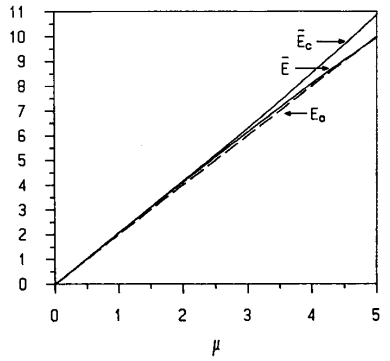

Fig. 12. Average soliton energy $\bar{E}$ versus μ. The average soliton energy obtained by CDA $\bar{E}_c$ and the initial soliton energy E_o are also shown.

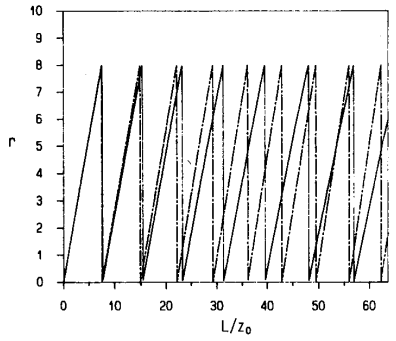

Fig. 13. Normalized phase change ratio r versus L/z_o where $r \equiv L/z_e$ (mod 8). The ratio obtained by CDA is shown by the dashed line.

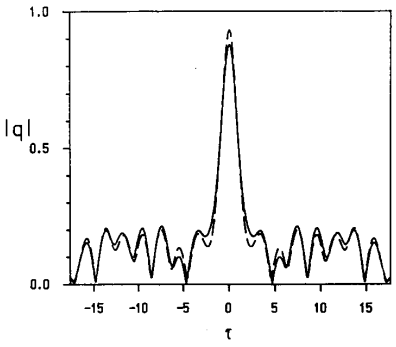

Fig. 14. Envelopes of the soliton ($|q|$) obtained by NCD and CDA (the dash line) for $\mu = 1$, $\xi_p = 4$ at $\xi = 200$ (2000 km).

the average energy of the soliton over the pump period. From (25), the effective soliton period can be defined as

$$z_e = (2\pi/\bar{E}^2)X. \tag{28}$$

The resonant peaks occurs when L/z_e is the multiple of 8 where the phase shift of the soliton is the multiple of 2π. Fig. 12 shows the average energy of the soliton in Fig. 11 where the result obtained by CDA is denoted by $\bar{E}_c$. In Fig. 12, the dashed line represents the initial energy E_o. It is seen that $\bar{E}_c > \bar{E}$ for all μ. Larger average energy corresponds to shorter effective soliton period or faster phase change. In Fig. 12, $\bar{E}_c > \bar{E}$ for all μ values, which means L/z_e obtained by CDA is larger than that obtained by NCD. This is the reason that, in Fig. 11, the resonant peaks obtained by CDA are advanced. We define the normalized phase change ratio $r \equiv L/z_e$ (mod 8). The resonance occurs when $r = 0$, which corresponds to the phase shift of the soliton is the multiple of 2π. Fig. 13 shows r versus L/z_o. It is found that the resonant peaks in Fig. 13 fit those in Fig. 11 well for $L/z_o < 40$. It is noticed that the resonant peaks obtained by NCD occur near the multiples of 7.5 rather than 8.0. The resonant peaks occur periodically because in Fig. 12 $\bar{E}$ is close to E_o. It is also found that in Fig. 11 the valleys occur when the phase shift of the soliton is the odd integer multiple of π. It is noticed that $\bar{E} < E_o$ for $\mu > 4.4$ where $\mu = 4.4$ corresponds to I_{oe} in Fig. 9.

Large δS corresponds to large pulse shape change of the soliton and unstable soliton propagation. To obtain stable soliton propagation, usually the region δS in Fig. 11 near and below zero is chosen. Fig. 14 shows the envelope of the soliton with $\mu = 1$ at $\xi = 200$ (2000 km) and that obtained by CDA for comparison. It is seen that the envelopes of the two solitons are almost the same. For smaller μ, not only the envelopes are more alike, but also the pulse qualities are better and the noise waves are reduced.

The other region in Fig. 11, the large positive δS region, corresponds to unstable soliton propagation. The resonant peaks in the region corresponds to the extrema of the unstability of the soliton propagation. The resonant peaks of the two curves are different. In some cases, the peak of one curve corresponds to the valley of the other curve. Figs. 15 and 16 show the evolution of the soliton with $\mu = 5$ for NCD and CDA, respectively. δS is at the valley for NCD and at the peak for CDA. It is seen that the soliton calculated by NCD can maintain its pulse shape well until 1120 km ($\xi = 112$), while the result calculated by CDA is only 520 km. On the contrary at $\mu = 4.82$ where δS is at peak for NCD and at valley for CDA,

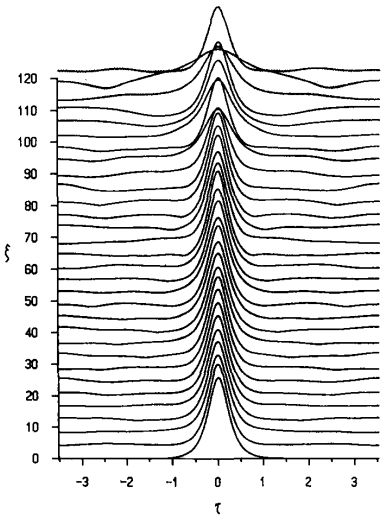

Fig. 15. Envelope evolutions of the soliton for $\mu = 5$, $\xi_p = 4$ with NCD. The initial pump intensity $I_o = 5.1094$.

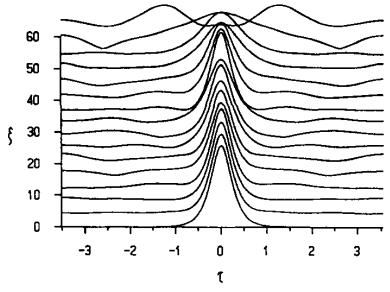

Fig. 16. Envelope evolutions of the soliton for $\mu = 5$, $\xi_p = 4$ with CDA. The initial pump intensity $I_o = 5.1373$.

the soliton calculated from CDA can be maintained better. The propagation distance over which the soliton with CDA can still maintain its pulse shape is 640 km, while that with NCD is only 440 km.

VI. Conclusion

In this paper, we have shown a numerical method to solve the coupled equation of the soliton and Raman pump waves. In this method, we only assume a large relative velocity between the soliton and Raman pump wave. For bidirectional Raman pumps, both forward and backward pump depletion rates can be obtained. In literature, they are assumed to be constant. It is found that the constant depletion approximation is valid for small depletion rate, which requires low soliton power (or long pulsewidth), small material loss and a short pump period.

In periodically Raman-pumped fiber, a stable signal energy exists. The signal energy is the total energy that includes the soliton energy and the noise energy. The noise is radiated out from the soliton due to the perturbation of the combined effect of the fiber loss and Raman gain. The relation of the stable signal energy and pump intensity is obtained. It is found that stable signal energy is very sensitive to the pump intensity. A slight change of the pump intensity may cause a large change in the signal energy. The stability of the soliton propagation in the Raman-pumped fiber is also studied. It is found that the stability predicted by NCD and CDA are generally different.

References

[1] A. Hasegawa and Y. Kodama, "Signal transmission by optical solitons in monomode fiber," *Proc. IEEE*, vol. 69, pp. 1145–1150, Sept. 1981.
[2] A. Hasegawa, "Numerical study of optical soliton transmission amplified periodically by the stimulated Raman process," *Appl. Opt.*, vol. 23, pp. 3302–3309, Oct. 1984.
[3] L. F. Mollenauer, J. P. Gordon, and M. N. Islam, "Soliton propagation in long fibers with periodically compensated loss," *IEEE J. Quantum Electron.*, vol. QE-22, pp. 157–173, 1986.
[4] S. Chi and S. Wen, "Interaction of optical solitons with a forward Raman pump wave," *Opt. Lett.*, vol. 14, pp. 84–86, Jan. 1989.
[5] L. B. Jeunhomme, *Single-Mode Fiber Optics*. New York: Dekker, 1983, p. 257.
[6] K. Mochizuki, "Optical fiber transmission systems using stimulated Raman scattering: theory," *J. Lightwave Technol.*, vol. LT-3, pp. 688–694, June 1985.
[7] D. Yevick and B. Hermansson, "Soliton analysis with the propagation beam method," *Opt. Comm.*, vol. 47, pp. 101–106, Aug. 1983.
[8] L. F. Mollenauer and K. Smith, "Demonstration of soliton transmission over more than 4000 km in fiber with loss periodically compensated by Raman gain," *Opt. Lett.*, vol. 13, pp. 675–677, Aug. 1988.

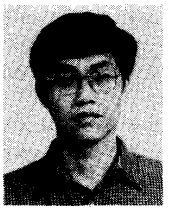

Senfar Wen was born on July 29, 1961, in Fengyuan, Taiwan, Republic of China. He received the B.S. degree in electro-physics, the M.S. degree in electro-optical engineering, and the Ph.D. degree in electro-optical engineering, all from National Chiao Tung University, Taiwan, in 1983, 1985, and 1989, respectively.

He is currently a post-doctoral Fellow at the Center for Telecommunications Research, National Chiao Tung University, working in the area of the nonlinear effects in optical fiber and their applications to optical communications.

Tsun-Yee Wang was born on November 3, 1950, in Tainan, Taiwan, Republic of China. He received the B.S. degree in electronic engineering and the M.S. degree in electronic engineering, both from National Chiao Tung University, Taiwan, in 1973 and 1975, respectively.

He is presently engaged in research on optical fiber communication for his Ph.D. degree at National Chiao Tung University, Taiwan.

Sien Chi was born on July 6, 1936, in Huaiying, Jiangsu, China. He received the B.S.E.E. and M.S.E.E. degrees from National Chiao Tung University, Taiwan, China, in 1959 and 1961, respectively. He received the Ph.D. degree in electrophysics from the Polytechnic Institute of Brooklyn, Brooklyn, NY, in 1971.

In 1971, he joined the faculty of National Chiao Tung University, where he is currently a Professor of electro-optical engineering. From 1977 to 1978 he was a Resident Visitor at Bell Laboratories, Holmdel, NJ. From 1986 to 1987 he took a sabbatical leave to Hua Eng Wires and Cables, Taiwan, where he conducted research programs in fiber optics. His research interests are in the area of fiber and nonlinear optics.